Available online at www.sciencedirect.com
ScienceDirect
Journal of the European Ceramic Society 28 (2008) 2085–2098
www.elsevier.com/locate/jeurceramsoc

New production of TiC_xN_{1-x}-based cermets by one step mechanically induced self-sustaining reaction: Powder synthesis and pressureless sintering☆

J.M. Córdoba*, M.D. Alcalá, M.A. Avilés, M.J. Sayagués, F.J. Gotor

Instituto de Ciencia de Materiales de Sevilla, Centro mixto CSIC-US, Av. Américo Vespucio 49, 41092 Sevilla, Spain

Received 26 November 2007; received in revised form 28 January 2008; accepted 1 February 2008
Available online 3 April 2008

Abstract

TiC_xN_{1-x}-based powdered cermets were synthesized by a one step mechanically induced self-sustaining reaction (MSR) process from mixtures of elemental powders, and subsequently sintered by a pressureless method. The composition and microstructure of the ceramic and binder phases before and after the sintering process were studied by X-ray diffraction, scanning and transmission electron microscopy, and electron diffraction. The powdered cermets showed excellent binder dispersion and a nanometer character for the ceramic and binder particles. The TiC_xN_{1-x} stoichiometry was consistently richer in carbon than expected from the raw powder composition. An important amount of titanium was present in the binder after MSR synthesis, and intermetallic Ti–Ni or Ti–Co phases were obtained in some cases. After sintering, the binder phase was always constituted by intermetallic compounds. The morphology of the ceramic phase in the final bodies was dependent on the C/N ratio of TiC_xN_{1-x} and its growth primarily occurred through a coalescence process. The presence of titanium in the binder reduced hard particle solubility in the melted binder and its grain growth.

Keywords: Ti(C, N); Cermets; Mechanical activation; Sintering; SHS

1. Introduction

Cermets are generally made of Ti(C, N) solid solution (or mixtures of TiC and TiN) as the main hard component and Co or/and Ni as the binder. A variety of binary carbides such as Mo_2C, WC, TaC or NbC are added to improve the sinterability, hot hardness and thermal shock resistance of cermets.[1] They are produced by sintering a compacted powder mixture at a temperature where a liquid phase is formed. The final microstructure consists of hard ceramic grains embedded in a tough metallic binder. It has been shown that the shape and size of ceramic particles are dependent on the C/N ratio.[2,3] When several ceramic components are employed, the typical core–rim microstructure for the hard phase is developed. The core corresponds to undissolved titanium carbonitride, while the rim corresponds to complex carbonitride solid solutions containing titanium and other heavier elements such as Mo, W, Ta or Nb. The rim phases that surround the core are formed through a dissolution–reprecipitation process in the liquid melt. In some cases, the rim microstructure appears divided into an inner and outer rim with different chemical compositions. The chemical composition and microstructure of Ti(C, N)-based cermets are therefore heterogeneous and rather complex due to the wide variety and quantities of hard components and metallic binder systems.[1,4]

Cermets based on titanium carbonitride are currently used in a wide variety of cutting tool applications due to their excellent combination of mechanical properties.[1,4,5] They have improved surface finishing, ensuring at the same time excellent chip and tolerance control, and the dimensional accuracy of workpieces compares with WC–Co conventional tools.[6,7] Despite being a good candidate to substitute WC–Co in structural applications,[8] nowadays, its applications are restricted to high-speed finishing and cutting operations due to its high thermal conductivity that results in less thermal stress and cracks. These cermets also exhibit excellent wear resistance and chemical stability at high temperatures.

☆ Supported by the Spanish Government under Grant No. MAT2006-04911.
* Corresponding author.
E-mail address: jmcordoba@icmse.csic.es (J.M. Córdoba).

0955-2219/$ – see front matter © 2008 Elsevier Ltd. All rights reserved.
doi:10.1016/j.jeurceramsoc.2008.02.007

The development of new cutting tool inserts in industrially developed countries is continuous and remains an issue. In particular, great efforts are being made to improve the toughness of Ti(C, N) cermets so that they become a feasible alternative to WC–Co hard metals.[9] Different routes have been explored in order to achieve this goal, such as modifying the nature and the alloy status of the prematerials,[10] improving sintering technologies or employing ultrafine powders with better homogeneity of the constituent phases.[11] This last strategy has the disadvantage of high cost for raw materials that considerably increases the final price of the product.

Mechanical milling has shown to be a powerful powder processing technique that allows production of cost-effective ultrafine products (even nano-structured materials) and extremely homogenous composite materials.[12] In addition, it is a solvent-free and low temperature process. Powders obtained by this synthetic method have high sinterability due to the refined microstructure and the great amount of induced defects. Thus, mechanical milling is often used to activate the reactants before a subsequent annealing or sintering treatment.[13–15] In general, milled powders react faster and a lower temperature is required. Sometimes, a combination of mechanical milling and self-propagating high-temperature synthesis (SHS) has been employed. The microstructure of powder mixture is modified by milling and then the SHS reaction is initiated by pressing the powder into a pellet and igniting it.[16,17] The milling step can progressively reduce the ignition temperature by increasing the milling time. It has been also shown that SHS can be induced at room temperature by exposing mechanically activated metal-graphite powder mixtures to air and has been successfully applied to the synthesis of carbides, nitrides and borocarbides.[18]

Concerning reactive milling processes, e.g., mechanical milling accompanied by a solid-state reaction, it has been shown that if induced reactions by milling are exothermic enough, a self-sustaining reaction similar to SHS can be initiated after a critical milling time.[19] One can imagine that prolonged milling as previously described for SHS can reduce the ignition temperature to room temperature and a spontaneous mechanically activated SHS reaction is achieved within the milling vial. This kind of mechanochemical process is generally called mechanically induced self-sustaining reaction (MSR) as proposed by Yen et al.[20] MSR could be suitable to produce TiC_xN_{1-x}-based cermets because it has been presented as a novel method to produce high purity transition metal carbonitrides from mixtures of elemental transition metals and carbon in a nitrogen atmosphere.[21–23] In addition, MSR permitted to obtain nanocrystalline carbonitride powders with homogeneous and controlled chemical composition (tailored C/N ratio) by adequately adjusting the milling parameters and the metal-to-carbon atomic ratio in the starting mixture.

This work is the first attempt to employ MSR as an alternative procedure to be used in the fabrication of TiC_xN_{1-x}-based cermets by a new, simple, direct and effective way. The sintering behaviour of powdered cermets synthesized by MSR process was also studied. We have evaluated the microstructural characteristics of the sintered material and focused on changes in chemical composition of hard and binder phases during the liquid phase sintering. We have attempted to determine a relationship between the raw powder characteristics and the final microstructure of cermets.

2. Experimental

Titanium powder (99% in purity, <325 mesh, Strem Chemicals), graphite powder (<270 mesh, Fe ≤ 0.4%, Merck), cobalt powder (99.9% in purity, <100 mesh, Sigma), nickel powder (puriss., Fluka), tungsten powder (99.95% in purity, Strem Chemicals), tungsten carbide powder (WC, 99.5% in purity, <1 μm, Strem Chemicals) and molybdenum carbide powder (Mo_2C, 99.5% in purity, Strem Chemicals) were used in this work.

The different powder mixtures were ball milled under 6 atm of high-purity nitrogen gas (H_2O and $O_2 \leq 3$ ppm, Air Liquide) using a modified planetary ball mill (model Vario-Planetary Mill Pulverisette 4, Fritsch) at a spinning rate of 400 rpm for both the rotation of the supporting disc and the superimposed rotation in the direction opposite to the vial. Fifteen tempered steel balls, together with 46.5 g of reactive powder (except for sample C3), were placed in a tempered steel vial (67Rc) for each milling experiment. The volume of the vial was 300 ml. The diameter and weight of balls were 20 mm and 32.6 g, respectively. The powder-to-ball mass ratio (PBR) was 1/10.5 (except for sample C3, PBR of 1/21). The vial was purged with nitrogen gas several times, and afterward the desired nitrogen pressure (6 atm) was selected before milling. The vial was permanently connected to the gas cylinder during milling experiments by a rotary valve and a flexible polyamide tube. The pressure was continuously monitored by a SMC Solenoid Valve (model EVT307-5DO-01F-Q, SMC) connected to a data acquisition system ADAM-4000 series (Esis Pty Ltd.). The self-sustaining reaction inside the vial was detected from the time–pressure value monitored during milling. This record displayed a peak when the ignition took place due to the heat generated by the highly exothermic reaction.

Cermets were fabricated through a pressureless process. Powdered cermets were first shaped (green bodies) and then sintered at high temperature to obtain hard cermets. The forming process was performed by means of cold isostatically pressing at 200 MPa for 5 min to yield cylinders of 12 mm of diameter and 45 mm in height. The green bodies were sintered at 1400 °C for 60 min (heating rate 10 °C/min, free cooling) under inert atmosphere (helium gas, $H_2O \leq 3$ ppm, $O_2 \leq 2$ ppm and $C_nH_m \leq 0.5$ ppm, Air Liquide) in a horizontal furnace (Thermolyne Type 59300 model no. F-59340-CM, Thermolyne).

X-ray diffraction patterns of powders and polished surfaces of cermets were obtained with a Philips X'Pert Pro instrument equipped with a Θ/Θ goniometer using Cu Kα radiation (40 kV, 40 mA), a secondary K_β filter, and an X'Celerator detector. The diffraction patterns were scanned from 30° to 130° (2Θ) at a scanning rate of 0.42° min^{-1}. Silicon powder (NIST) was used to correct XRD shift peaks. Lattice parameter, a, of TiC_xN_{1-x} phases was calculated from the whole set of peaks of the XRD diagram by using the Fullprof computer program assuming a cubic symmetry.[24] The composition (x) of TiC_xN_{1-x} solid

solution was estimated from Vegard's law obtained from the following JCPDS data files: TiN (38-1420), $TiC_{0.3}N_{0.7}$ (42-1488), $TiC_{0.7}N_{0.3}$ (42-1489), and TiC (32-1383).

Microstructural characterization was carried out by using scanning and transmission electron microscopy. Scanning electron microscopy (SEM) images were obtained by a Philips XL-30 microscope equipped with an Oxford-Link X-ray analysis system. Transmission electron microscopy (TEM) images and electron diffraction (ED) patterns were taken on a 200 kV Philips CM200 microscope with a supertwin objective lens and a LaB_6 filament (point resolution ~0.25 nm). High-resolution scanning electron microscopy (HRSEM) experiments were performed in a Hitachi S5200 microscope. Powder samples were dispersed in ethanol and droplets of the suspension were deposited onto a holey C film. For the TEM and HRSEM characterization of consolidated cermets, thin disks (3 mm Ø) were prepared by a process of subsequent cutting, polishing, dimpling and finally ion milling (DuoMill, Gatan Inc.).

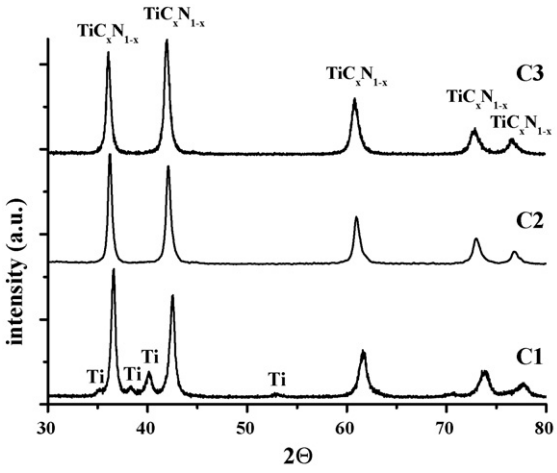

Fig. 1. XRD patterns of C samples after MSR process.

3. Results and discussion

3.1. Powder synthesis

To provide an insight into the MSR process leading to the powdered cermets, three samples constituted only of the ceramic phase (without metallic binder) were obtained from titanium and graphite mixtures (samples labelled as C in Table 1). Half the amount of starting mixture was employed for sample C3 because of the high exothermicity of the process caused extreme overpressure. Fig. 1 shows the XRD patterns corresponding to these three samples. The formation of a titanium carbonitride phase by a combustion process was observed in the three cases. Ignition times, which were determined from the time–pressure value recorded during milling, have been included in Table 1. The shift noticed in XRD peaks (Fig. 1), as has been proved in previous works,[21,22] is attributed to different stoichiometries (C/N ratio) for the TiC_xN_{1-x} phase. Unreacted Ti was also observed in sample C1, which possessed the lowest graphite content in the starting mixture, and was evidence for an incomplete combustion. This fact is in agreement with previous results on transition metal carbonitrides that showed a lack of combustion for mixtures with low carbon contents.[22] Iron contamination coming from the milling media (vial and balls) was not detected in XRD patterns. In a previous work,[21] an iron content of ~1–2 wt% was determined by titration in TiC_xN_{1-x} products obtained by MSR.

Powdered cermets were prepared by MSR in a nitrogen atmosphere starting from elemental powders: titanium and graphite necessary for TiC_xN_{1-x} formation, and nickel or cobalt as the binder phase. In some cases, a third phase such as W, WC or Mo_2C was added to the initial mixture before milling. Different starting mixtures are shown in Table 1 and were labelled as PC. A combustion process took place in all mixtures and ignition times are also shown in this table. Milling time after ignition was held ~30 min in order to normalize the milling process and obtain a homogeneous product. The XRD patterns of these powdered cermets obtained by MSR (Fig. 2) show the formation of the TiC_xN_{1-x} phase. XRD peaks of TiC_xN_{1-x} also exhibit the typical shift due to a different C/N ratio in its stoichiometry. Adding to the initial titanium/graphite mixture up to 20 wt% of phases (binder and additives) that did not participate in the MSR process did not inhibit the TiC_xN_{1-x} formation by a combustion reaction. The ignition time increased ~10 min due to the presence of these phases, which were considered inert regarding the titanium/graphite mixture. In particular, ductile nickel and cobalt can absorb part of the energy provided by the mill trough ball–ball and ball–wall impacts. All energy transmitted by the

Table 1
Milling conditions for different powdered ceramics (C) and cermets (PC)

Sample	Raw powders Ti/C (atomic ratio) + binder (wt%) + 3rd phase (wt%)	No. balls (PBR)	N_2 (atm)	v (rpm)	Ignition time (min)
C1	Ti/C (1/0.25)	15 (1/10.5)	6	400	32
C2	Ti/C (1/0.5)	15 (1/10.5)	6	400	30
C3	Ti/C (1/0.75)	15 (1/21)	6	400	24
PC1	Ti/C (1/0.25) + Ni (15%)	15 (1/10.5)	6	400	45
PC2	Ti/C (1/0.5) + Ni (15%)	15 (1/10.5)	6	400	39
PC3	Ti/C (1/0.75) + Ni (15%)	15 (1/10.5)	6	400	48
PC4	Ti/C (1/0.5) + Co (15%)	15 (1/10.5)	6	400	42
PC5	Ti/C (1/0.5) + Ni/Co (7.5%/7.5%)	15 (1/10.5)	6	400	40
PC6	Ti/C (1/0.5) + Co (15%) + W (5%)	15 (1/10.5)	6	400	39
PC7	Ti/C (1/0.5) + Co (15%) + WC (5%)	15 (1/10.5)	6	400	37
PC8	Ti/C (1/0.5) + Co (15%) + Mo_2C (5%)	15 (1/10.5)	6	400	40

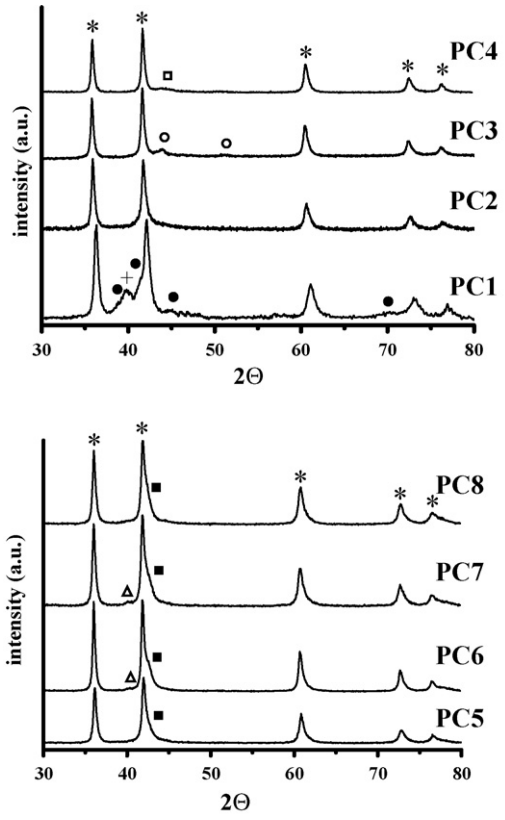

Fig. 2. XRD patterns of PC samples after MSR process. (*) TiC_xN_{1-x}; (□) (Co, Ti); (◯) (Ni, Ti); (●) Ti_2Ni; (+) Ti; (■) CoTi; (△) W.

milling device was not transferred to the reactive Ti/C mixture and, consequently, the ignition was delayed.

The metallic binder is hardly detected in XRD patterns of powdered cermets (Fig. 2). The small amount of metal in the starting mixture along with milling effects, which induce crystalline refinement and lattice strains, were responsible for the small XRD peak intensity. A small particle size increases the difficulty in detecting metal and alloys by XRD, and a larger amount of material is required when particle size is in the submicrometric range. For example, it has been shown in Ti–Al mixtures that while 2 wt% of Ti can be easily detected if the particle size is in the range of 26–38 μm, about 25 wt% of Ti is needed if the particle size is in the range of 50–1000 nm.[25] In this sense and as it is shown in Fig. 4d where the dark field TEM image of a representative powdered cermet is presented, the particle size of the metallic binder (bright contrast) had a nanometric character with a particle size ranging between 5 and 15 nm.

Nickel and cobalt were not only inert regarding the MSR titanium carbonitride synthesis delaying ignition time, but also extracted titanium from the titanium/graphite mixture. The presence of (Co, Ni)–Ti intermetallic phases was observed in some of the powdered cermets (Fig. 2): CoTi in samples PC5–PC8, and Ti_2Ni in sample PC1. The formation of this last intermetallic phase in sample PC1 could be explained by looking at the XRD pattern of sample C1 (Ti/C atomic ratio of 1/0.25 without metallic binder). This pattern showed the existence of a non-negligible amount of unreacted titanium (incomplete combustion) after the MSR effect. The same behaviour would be expected in sample PC1 and the formation of a Ti-rich intermetallic phase was favoured in presence of Ni. In powdered cermets PC2–PC4, XRD peaks for Ni and Co were shifted to lower 2θ angles, which was related to an increased lattice parameter probably due to the formation of (Ni, Ti) or (Co, Ti) solid solutions. X-ray diffraction of powder mixtures of Ni and Ti milled under similar conditions did not show any interaction between both metals, which suggests that the formation of intermetallic phases or solid solutions observed in PC samples was triggered by the heat released during the combustion process involved in the carbonitride phase formation.

It is interesting to note that XRD patterns in samples PC6–PC8 show the presence of elemental W and probably Mo, although in samples PC7 and PC8 these elements were introduced as WC and Mo_2C, respectively. It has been shown during liquid phase sintering of cermets that WC, W_2C and Mo_2C dissolved in the binder providing W or Mo and C to the sintering media.[26] The presence of W and Mo as ascertained by XRD confirms that the MSR method, although induced at room temperature, should be considered at least from a local point of view such as a high-temperature process. The high temperature reached inside the vial during MSR was also corroborated by the presence in sample PC4 of cubic cobalt, the high temperature form.

Lattice parameter for each carbonitride phase calculated using the Fullprof software is shown in Table 2. TiC_xN_{1-x} stoichiometry estimated applying the Vegard's law is also included in this table. As expected, TiC_xN_{1-x} stoichiometry in samples C1–C3 was clearly dependant on the starting Ti/C atomic ratio. These values were similar to that reported in a previous work[21] employing the same starting mixture but using a smaller milling device (Pulverisette 7). This result confirms that this kind of MSR process can be scaled up with high levels of reproducibility. On the other hand, the stoichiometry of TiC_xN_{1-x} in powdered cermets (samples PC1–PC8) was richer in carbon compared with that of samples obtained without a binder phase (samples C1–C3). This fact agrees with XRD patterns, where it was observed that some amount of titanium from the starting Ti/C mixture was employed to form intermetallic compounds or (Ni, Ti) and (Co, Ti) solid solutions. The highest enrichment in carbon was noticed in powdered cermet PC1 with the start-

Table 2
Lattice parameter (a) and stoichiometry of TiC_xN_{1-x} phase in C and PC samples

Sample	a (Å)	XRD composition
C1	4.2595	$TiC_{0.23}N_{0.77}$
C2	4.2995	$TiC_{0.66}N_{0.34}$
C3	4.3094	$TiC_{0.81}N_{0.19}$
PC1	4.2688	$TiC_{0.48}N_{0.52}$
PC2	4.3027	$TiC_{0.75}N_{0.25}$
PC3	4.3089	$TiC_{0.81}N_{0.19}$
PC4	4.2908	$TiC_{0.81}N_{0.19}$
PC5	4.2983	$TiC_{0.77}N_{0.23}$
PC6	4.2918	$TiC_{0.78}N_{0.22}$
PC7	4.2901	$TiC_{0.77}N_{0.23}$
PC8	4.2924	$TiC_{0.80}N_{0.20}$

ing Ti/C mixture lowest in carbon. This fact is in accordance with its XRD pattern that illustrated the presence of Ti_2Ni and unreacted Ti. In contrast, no carbon enrichment was observed for the powdered cermet with the highest graphite content (compare samples C3 and PC3 with a Ti/C atomic ratio of 1/0.75). In this case, the high amount of graphite in the starting mixture made the titanium-to-nickel contact more difficult hindering the formation of intermetallic or alloy phases.

Several authors have suggested during the synthesis of TiC–Ni cermets by SHS or MSR from elemental Ti, Ni and C powders that the presence of metallic elements (Ti, Ni) in the final product or others intermetallic phases depended on combustion and exothermic conditions.[27–29] The following exothermic reactions can be considered in our Ti–C–N–(Ni, Co) system:

$$2Ti + Ni \rightarrow Ti_2Ni, \quad \Delta H = -83\,kJ/mol$$

$$Ti + Ni \rightarrow TiNi, \quad \Delta H = -67\,kJ/mol$$

$$Ti + 3Ni \rightarrow TiNi_3, \quad \Delta H = -140\,kJ/mol$$

$$Ni + Co \rightarrow CoNi, \quad \Delta H = -3\,kJ/mol$$

$$Ti + Co \rightarrow TiCo, \quad \Delta H = -12\,kJ/mol$$

$$Ti + 3Co \rightarrow TiCo_3, \quad \Delta H = -42\,kJ/mol$$

$$Ti + C \xrightarrow{N_2} TiC_xN_{1-x},$$

$$\Delta H = \text{from} - 184\,kJ/mol\,(TiC)\,\text{to} - 338\,kJ/mol\,(TiN)$$

Assuming this consideration, intermetallic phases would appear in less exothermic systems and only a TiC_xN_{1-x} phase (thermodynamically more stable) with Ni or Co as diluent would be found in more exothermic ones. This presumed behaviour seems to occur in the Ti–C–N–(Ni, Co) system studied in this work. If we consider the peak height of the pressure–time record as a measurement of the exothermic character of the MSR process, we observed that this character was superior in those mixtures with a higher content of graphite. In this sense, when initial Ti/C atomic ratios higher than 1/0.5 were used, XRD patterns showed only the TiC_xN_{1-x} phase, without the formation of intermetallics. In sample PC1 (Ti/C 1/0.25), where the combustion was less energetic, the intermetallic Ti_2Ni phase appeared in the final product. In samples PC6–PC8, although a 1/0.5 (Ti/C) atomic ratio was employed, the presence of 5 wt% of W, WC or Mo_2C could contribute to diminishing the exothermic character of the reaction and the intermetallic CoTi phase was obtained.

A similar behaviour has been observed by Burkes et al.[30,31] during the synthesis of intermetallic-ceramic composites Ni_3Ti–TiC_x and NiTi–TiC by SHS under an inert atmosphere. For obtaining both composites, Ti/C atomic ratios less than 1 were always necessary and a higher exothermic character was observed when increasing carbon content. The synthesis was realized by adding free carbon to a starting Ti–Ni mixture. In our work, Ti/C atomic ratios <1 were also employed, but a reactive atmosphere of nitrogen was used. Under these experimental conditions, the starting atomic ratio had to be considered in our case as Ti/(C, N) ∼1, conditions that in principle must not favour the formation of intermetallic phases.

On the other hand, although the formation of Ti–Ni intermetallics is more exothermic than that of Ti–Co ones, CoTi phases were found in most of powdered cermets employing cobalt as a binder. Several authors have shown a high selectivity in mechanically induced combustion reactions when two reactions were initiated at the same time[32,33]; and the trend was to form those phases with the highest enthalpy formation values. Huang et al.[27] have assumed during the synthesis of TiNi–TiC composites by MSR that the formation of the intermetallic phase also occurs by a combustion process triggered by the heat released during the formation of the TiC phase. However, the fact that we have mainly observed the presence of Ti–Co and not Ti–Ni intermetallics in our products seems to suggest that these phases are not formed through a combustion process, but by another reaction mechanism. Assuming that during a MSR process extreme temperatures can be reached in local points of the vial and that this temperature can be higher than the melting point of the metal species involved in the reaction, the formation of metallic melts could be at the origin of the affinity between titanium and cobalt and its subsequent crystallization at the origin of the formation of CoTi phase. It is noteworthy that CoTi was only appreciated when a third metallic phase (Ni, W or Mo) was present in the media together with Co and Ti (samples PC5–PC8). This fact can be a consequence of the reduction of the temperature of formation of intermetallic melts when three different metals were present in the vial.

Representative SEM micrographs corresponding to samples PC2, PC5, PC7 and PC8 are shown in Fig. 3. SEM study revealed that the microstructure of products was similar and characteristic of samples obtained by MSR.[21–23] Powdered cermets were constituted of sub-micrometric particles highly agglomerated forming aggregates ranging between 1 and 5 μm. A representative TEM micrograph and the corresponding ED pattern of these powdered cermets are presented in Fig. 4a. Carbonitride particles are in fact polycrystalline as evidenced by the typical ED ring pattern. These particles consist of different nanodomains randomly oriented and ranging between 50 and 100 nm. The ED pattern can be indexed in the cubic system *Fm*-3*m* space group. With the purpose of observing the different phases (carbonitride and binder) in the powdered cermet, dark field and bright field were performed and representative images are presented in Fig. 4c and d, where the same area is compared. The nanometric metallic particles were well distributed in the whole sample, which will be extremely important for subsequent sintering processes. However, there were some particles where the binder was located preferably in the edge of these particles. This fact is in good agreement with EDX analysis that showed two different regions in terms of binder distribution (Fig. 4b).

3.2. Pressureless sintering

Two series of cermets were prepared (Table 3). The first one (HCB cermets) was obtained after sintering powder mixtures of the titanium carbonitride C2 sample (Ti/C atomic ratio 1/0.5) and

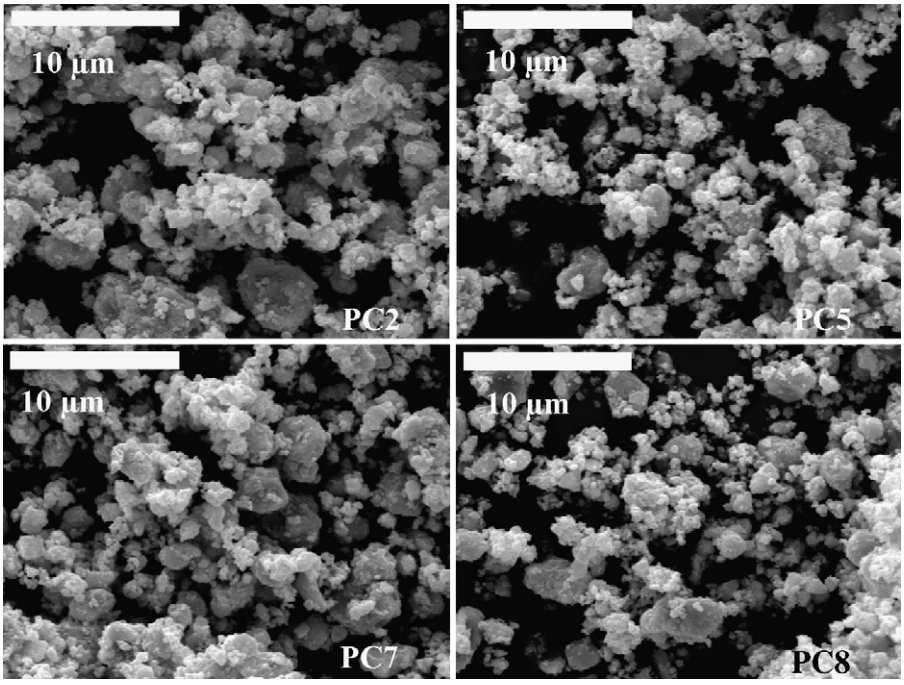

Fig. 3. SEM micrographs of samples PC2, PC5, PC7 and PC8 showing the typical morphology of samples obtained by MSR.

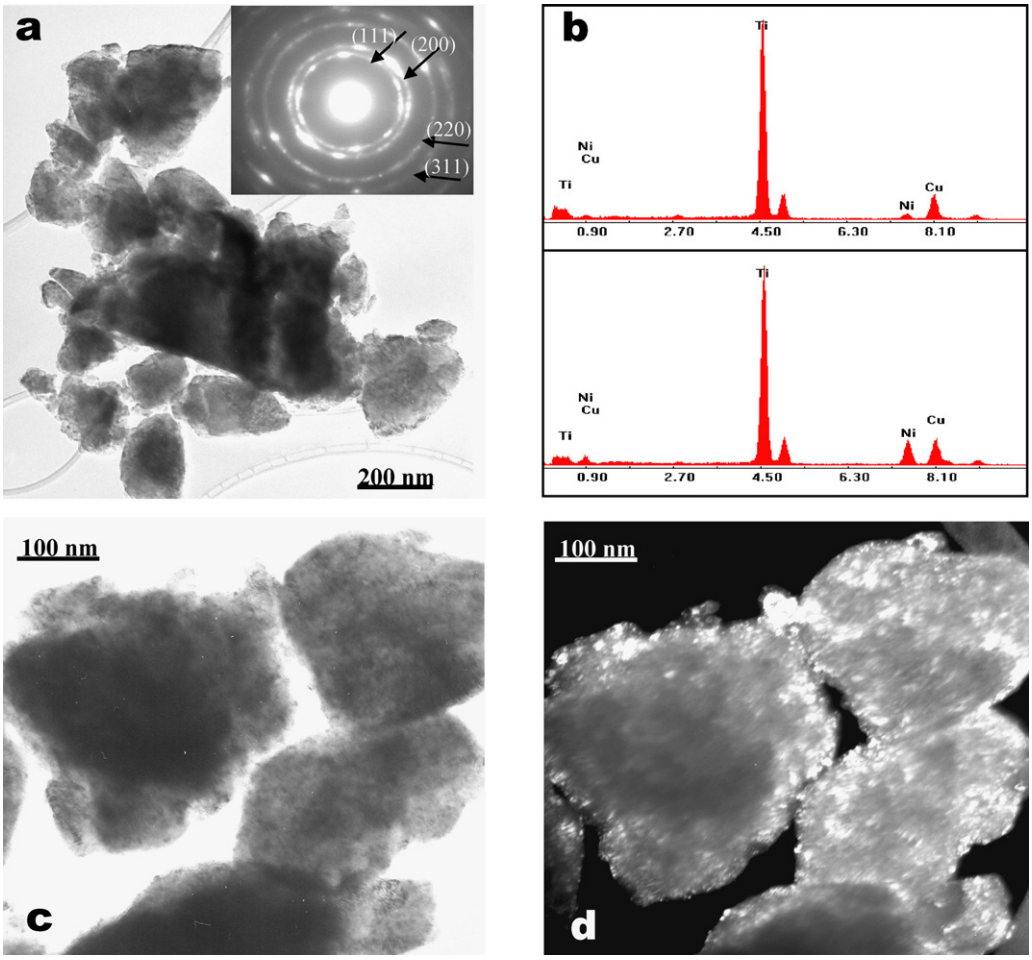

Fig. 4. (a) Representative TEM micrograph and the corresponding ED pattern of powdered cermets. All the indexed planes in the EDP correspond to the cubic carbonitride phase. (b) EDX analysis of two different areas in (a). (c) Bright and (d) dark field images of the same area.

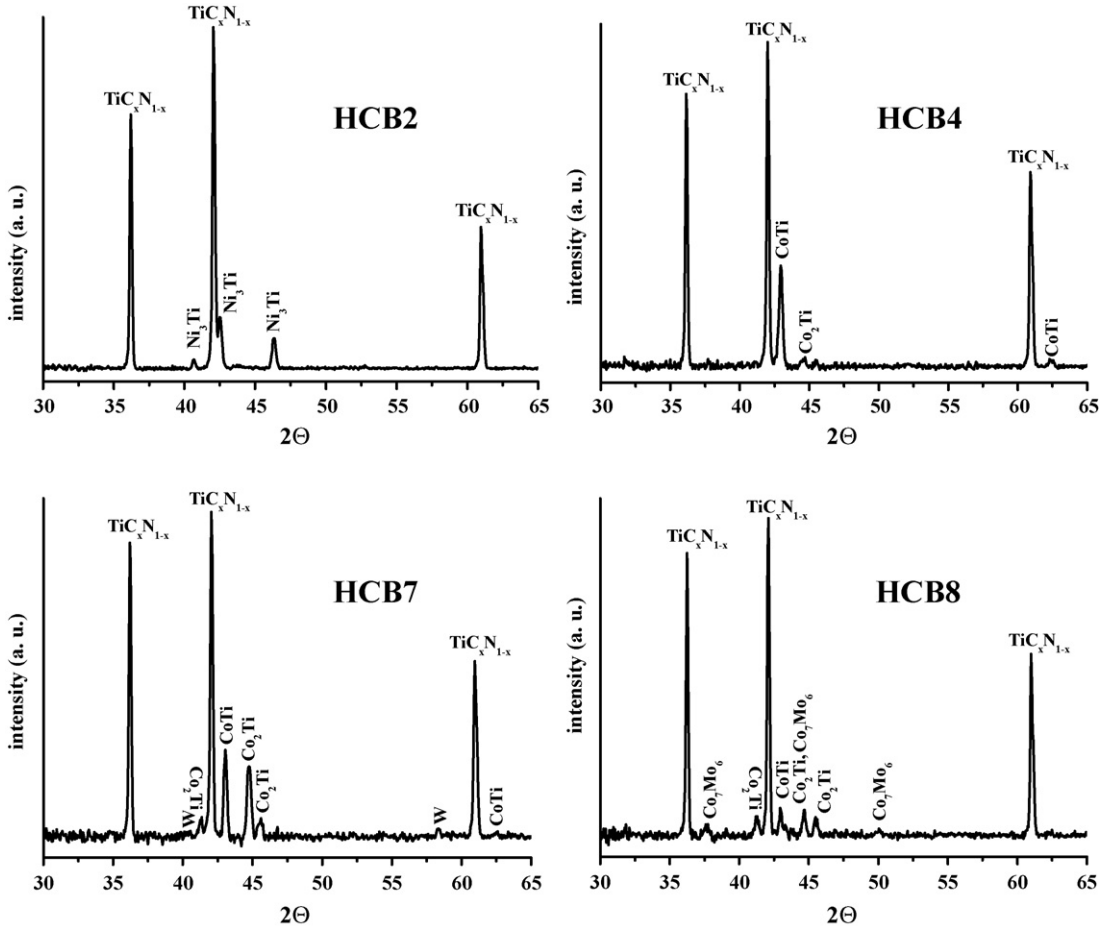

Fig. 5. XRD patterns of HCB cermets after sintering.

the metallic binder Ni or Co (HCB2 or HCB4 samples respectively). In some cases, a third phase WC or Mo_2C (HCB7 or HCB8 samples respectively) was added. The powder mixture was homogenized by sonication in ethanol for 10 min and afterwards in a centrifugal ball mill (Fritsch) for 60 min. The second series (HC cermets) corresponds to cermets sintered from the PC samples in Table 2, e.g., powdered cermets obtained by a one-step MSR process. The number of HCB cermets corresponds to the same gross composition of the raw materials as found in the HC ones.

XRD patterns of consolidated HCB cermets are shown in Fig. 5, where peaks for TiC_xN_{1-x} and metallic binder phases are observed. These binder phases were constituted of Ti–Ni or Ti–Co intermetallics produced during the high-temperature sin-

Table 3
Raw powders used for cermet fabrication (powder mixture subjected to MSR process marked by square brackets), lattice parameter (a) of TiC_xN_{1-x} phase, its stoichiometry, and binder phases present in sintered cermets

Cermets	Raw powders Ti/C (atomic ratio) + binder (wt%) + 3rd phase (wt%)	a (Å)	XRD composition	Binder phases
HCB2	[Ti/C (1/05)] + Ni (15%)	4.2967	$TiC_{0.70}N_{0.33}$	Ni_3Ti
HCB4	[Ti/C (1/0.5)] + Co (15%)	4.2982	$TiC_{0.69}N_{0.32}$	CoTi + Co_2Ti (m)
HCB7	[Ti/C (1/0.5)] + Co (15%) + WC (5%)	4.3004	$TiC_{0.71}N_{0.29}$	CoTi + Co_2Ti + W (m)
HCB8	[Ti/C (1/0.5)] + Co (15%) + Mo_2C (5%)	4.2970	$TiC_{0.67}N_{0.33}$	CoTi + Co_2Ti + Co_7Mo_6 (m)
HC1	[Ti/C (1/0.25) + Ni (15%)]	4.2705	$TiC_{0.36}N_{0.64}$	Ti_2Ni
HC2	[Ti/C (1/0.5) + Ni (15%)]	4.3037	$TiC_{0.75}N_{0.25}$	Ni_3Ti + (Ni, Ti)
HC3	[Ti/C (1/0.75) + Ni (15%)]	4.3071	$TiC_{0.79}N_{0.21}$	Ni_3Ti
HC4	[Ti/C (1/0.5) + Co (15%)]	4.3125	$TiC_{0.85}N_{0.15}$	Co_3Ti + (Co, Ti)
HC5	[Ti/C (1/0.5) + Ni/Co (7.5%/7.5%)]	4.3037	$TiC_{0.75}N_{0.25}$	(Co, Ni)Ti
HC6	[Ti/C (1/0.5) + Co (15%) + W (5%)]	4.3038	$TiC_{0.75}N_{0.25}$	CoTi + W (m)
HC7	[Ti/C (1/0.5) + Co (15%) + WC (5%)]	4.3033	$TiC_{0.74}N_{0.26}$	CoTi + W (m)
HC8	[Ti/C (1/0.5) + Co (15%) + Mo_2C (5%)]	4.3047	$TiC_{0.76}N_{0.24}$	CoTi + Mo (m)

(m): Minor phase.

tering process: Ni_3Ti in cermet HCB2, and CoTi and Co_2Ti in cermets HCB4, HCB7 and HCB8. Elemental Ni or Co was not observed after sintering. The presence of Ti-containing intermetallic phases in cermets was a clear evidence of TiC_xN_{1-x} dissolution in the binder during sintering. The formation of a Ti-richer intermetallic phase when Co instead of Ni was employed as binder indicated a higher solubility of TiC_xN_{1-x} in this melted metal. In cermets HCB7 and HCB8, small amounts of W and

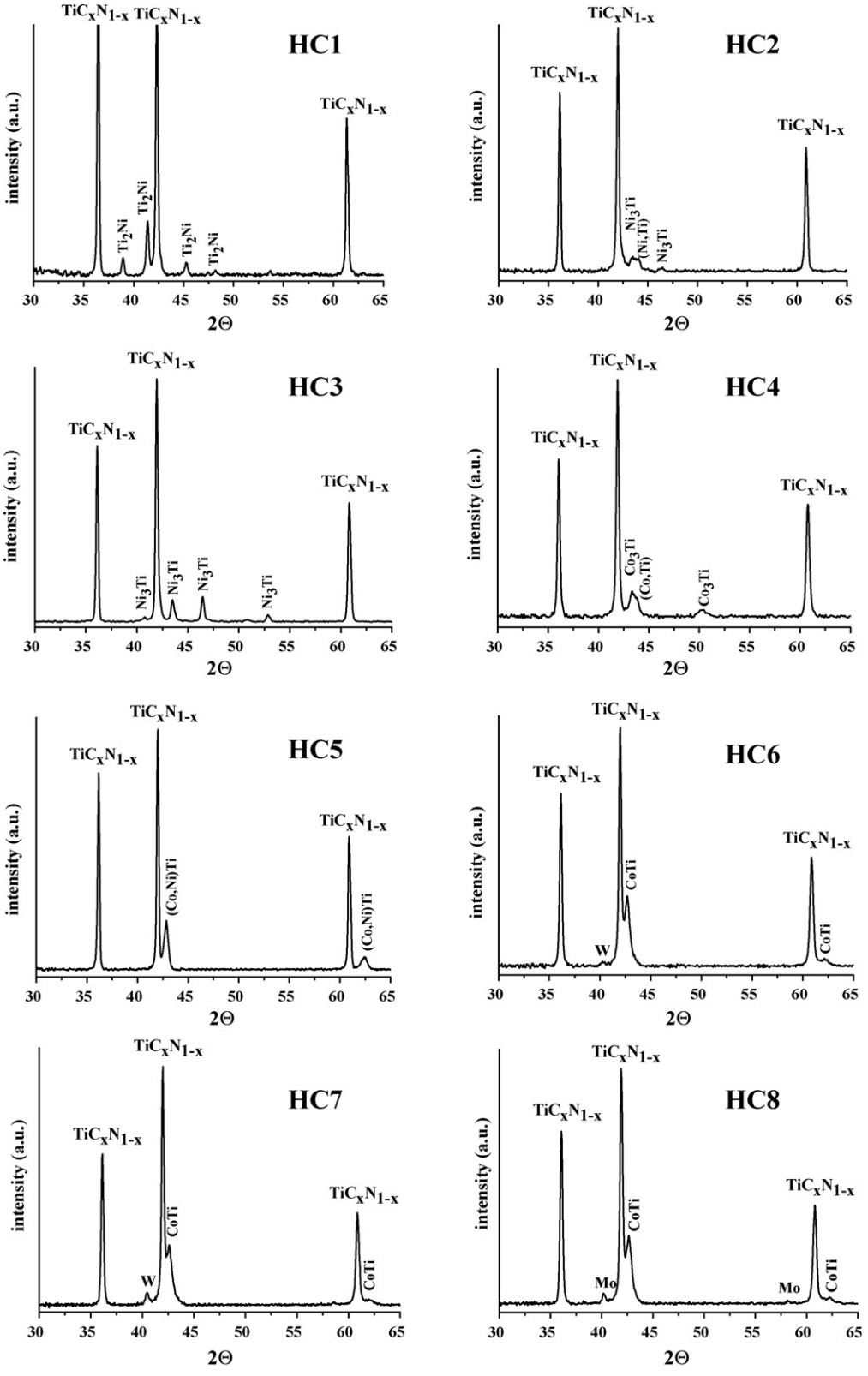

Fig. 6. XRD patterns of HC cermets after sintering.

Co_7Mo_6 were also detected, respectively, which indicated that WC and Mo_2C also dissolved and decomposed into the melted binder, which is in agreement with their high solubility values in Co (39 wt% at 1400 °C for both phases).[1]

XRD patterns of HC samples are shown in Fig. 6. These patterns show the presence of the carbonitride hard phase and intermetallic binder phases. Again, a tendency to primarily form CoTi and Ni_3Ti phases was observed when Co and Ni were added as metallic binder, respectively. If these XRD patterns are compared with those of powdered cermets obtained after the one-step MSR process (Fig. 2), two features can be outlined. First, if the intermetallic phase was produced during the MSR process, it remained following sintering (cermets HC1, HC5–HC8). Second, if only a shift in Ni or Co XRD peaks was observed after MSR (due to Ti dissolution in the metal structure), the intermetallic phase obtained after sintering was primarily γ′-Ni_3Ti or Co_3Ti (cermets HC2–HC4). It is interesting to note the presence of this γ′ phase because it has been shown in some reports that an improvement of tribological properties of Ti(C, N)-based cermets was possible when the γ′ phase (Ni_3M) was employed as binder.[34] This phase increases the creep resistance of cermets due to hardening of the binder by a precipitation pro-

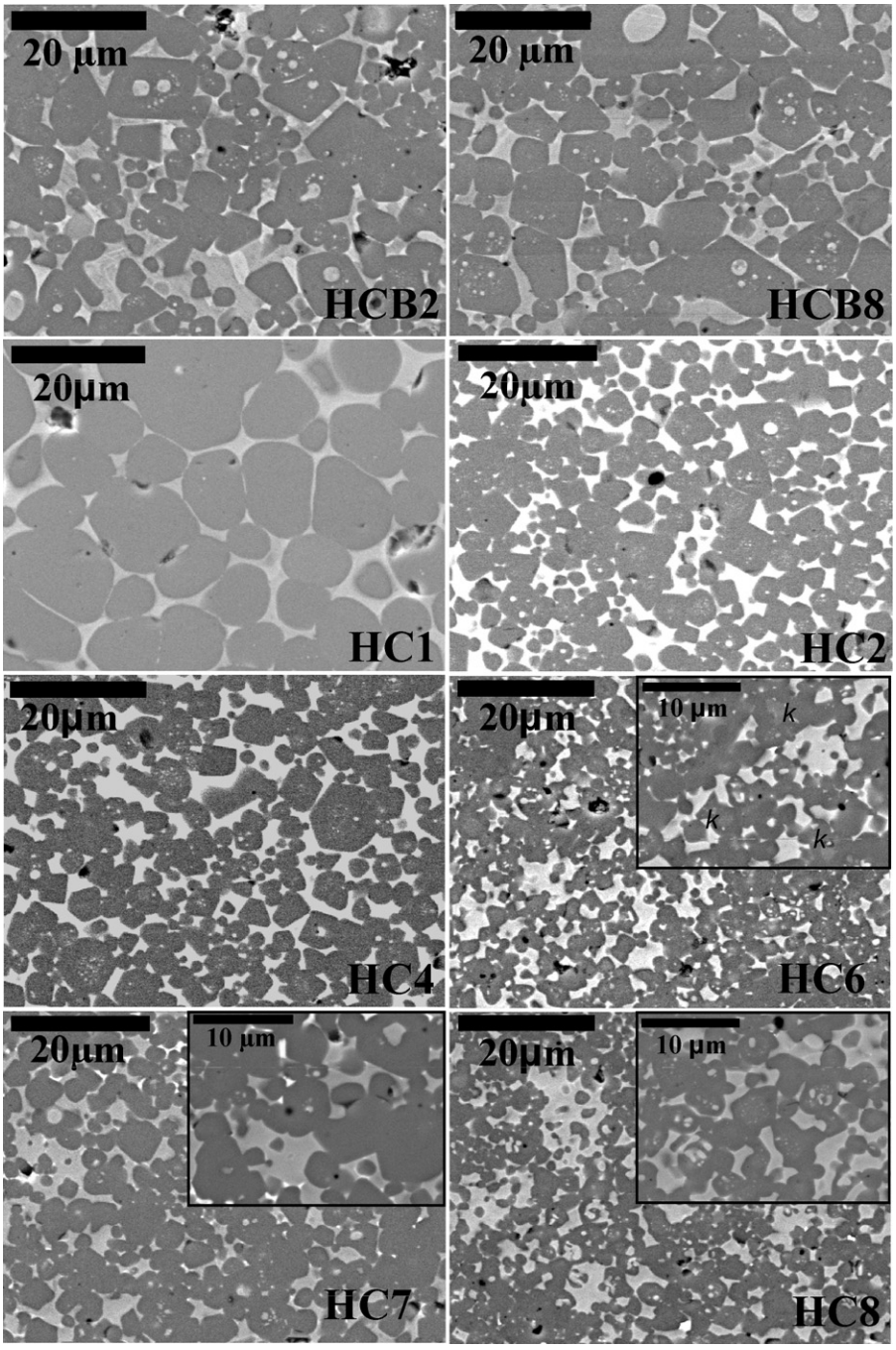

Fig. 7. SEM micrographs of selected HCB and HC cermets.

cess. Although a deleterious effect would be expected for high contents of γ' phase, Tiegs et al.[35,36] have shown good values of hardness and toughness by adjusting adequately the gross composition in TiC–Ni_3Al cermets.

Dissolution of the TiC_xN_{1-x} hard phase during sintering must be affected by the composition of the liquid binder. In this sense, a higher dissolution is expected when Ni or Co is added after MSR process (HCB cermets) because there is no Ti in the binder prior to sintering. This effect was highlighted by compositional changes observed in titanium carbonitride phase after sintering. Lattice parameter and stoichiometry for TiC_xN_{1-x} in all cermets (HC and HCB) are presented in Table 3. The nature of binder phases as observed by XRD is also shown. Two tendencies were observed by comparing compositional data of TiC_xN_{1-x} phase in Tables 2 and 3. In HCB cermets from powdered samples without titanium in the binder, a titanium carbonitride phase slightly richer in carbon was obtained after sintering. However, in HC cermets with titanium in the binder before sintering, the resulted titanium carbonitride after sintering was generally poorer in carbon.

These changes in TiC_xN_{1-x} stoichiometry cannot be explained in terms of different thermodynamic stability of carbon and nitrogen because titanium has a similar affinity for carbon and nitrogen at high temperature, as have been shown by Kang et al.[37,38] The high temperature stability of TiC_xN_{1-x} has been confirmed in a titanium carbonitride monolithic sample that did not show any compositional change after being heated at 1700 °C for 3 h under an inert atmosphere. Thus, it is clear that different behaviour observed in HC and HCB cermets regarding changes in TiC_xN_{1-x} stoichiometry was due to differences in TiC_xN_{1-x} dissolution in the binder during sintering. Ceramic phase dissolution in melted binder occurs through decomposition, as its elemental constituents incorporated to the liquid phase. Therefore, these stoichiometric changes observed during sintering can be explained taking into account the fact that titanium has higher solubility values than carbon (nitrogen solubility in the melted binder is practically negligible), and that titanium was present in the binder before sintering for HC cermets.

SEM micrographs of selected HCB and HC cermets are shown in Fig. 7. HCB cermets reveal a microstructure with small rounded particles and large particles with angular shape. Binder phase was located inside big faceted particles suggesting that they have grown from small ones by a coalescence process. Evidences of such growth can be observed in different regions of SEM micrographs. Hard particle microstructure does not seem to be affected by binder composition. Although, as shown in Fig. 4, TiC_xN_{1-x} phase obtained by MSR had a nanometric character, the microstructure as observed by SEM did not show nano-sized particles. This is not surprising because sharp increase in grain growth to micrometric level has been frequently observed during conventional sintering when densities close to the theoretical maximum are reached in systems with nanocrystalline particles.[39]

Leaving aside the microstructure of cermet HC1 that will be discussed later, SEM micrographs of HC cermets also show a bimodal character for the microstructure of hard ceramic (small rounded and larger faceted particles). A growth by coalescence seems also to occur in these cermets (the binder phase was observed inside hard particles); however the overall particle size was clearly smaller. This is illustrated in Fig. 8, where the TiC_xN_{1-x} particle size distribution for HCB2 and HC2 cermets is presented. For the HC cermet series, ceramic particle size appeared to diminish when a third phase was added (Fig. 7). It has been shown in TiC–Ni and Ti(C, N)–Ni cermets that original fine grains grow by coalescence in the early stages of sintering followed by a solution–reprecipitation mechanism.[2] Differences found in HCB and HC cermets can be explained if the solution–reprecipitation mechanism was hindered by the presence of a high amount of titanium in the melted binder that reduced considerably the solubility of hard particles in HC cermets. This effect was enhanced by W, WC or Mo_2C addition as these phases having a high solubility in liquid metallic binder.

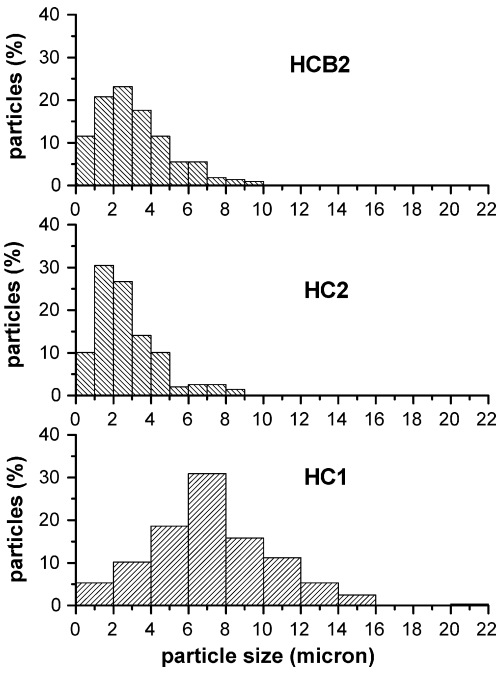

Fig. 8. Particle size distribution of TiC_xN_{1-x} in cermets (a) HCB2, (b) HC2, and (c) HC1.

Cermets HC6–HC8 with W, WC and Mo_2C additions, respectively, presented a less homogeneous distribution of binder phase (Fig. 7). Regions where binder was prominent over hard ceramics were observed, and it must be a consequence of the presence of these added phases with high solubility. Small bright areas observed in SEM micrographs corresponded to metallic W or Mo as ascertained by EDX analysis. Cermet HC8 showed the smallest ceramic particle size, in agreement with previous work where the inhibition of hard particle growth by Mo was shown.[40] Typical core–rim microstructure of cermets containing W- or Mo-phases was not observed due to the small amount of additives employed. However, in cermet HC6 where tungsten was added in its metallic form, some hard particles showed zones with different contrast, marked with *k* in Fig. 7. EDX analysis of these regions (Fig. 9) suggests that the lighter contrast could be

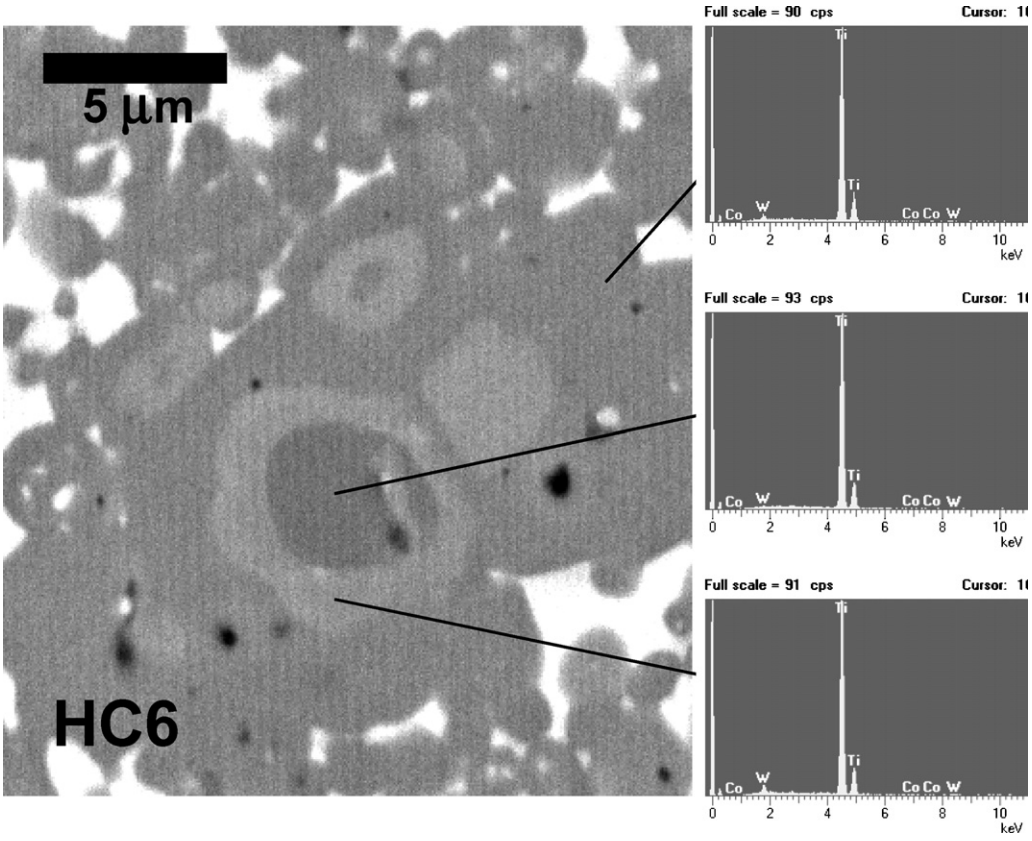

Fig. 9. SEM micrograph of cermet HC6 showing hard particles with lighter contrast, and EDX analysis in different regions of this cermet.

associated with the presence of (W, Ti)(C, N) solid solutions. In these particles, this contrast observed was, in some cases, similar to the typical core–rim microstructure but, in other cases, the contrast between the core and rim was inverted (lighter contrast for the core). This inversion can be produced in regions with high local concentrations in tungsten.

Cermet HC1 showed a different particle morphology, size and distribution for the hard ceramic (Figs. 7 and 8). Large

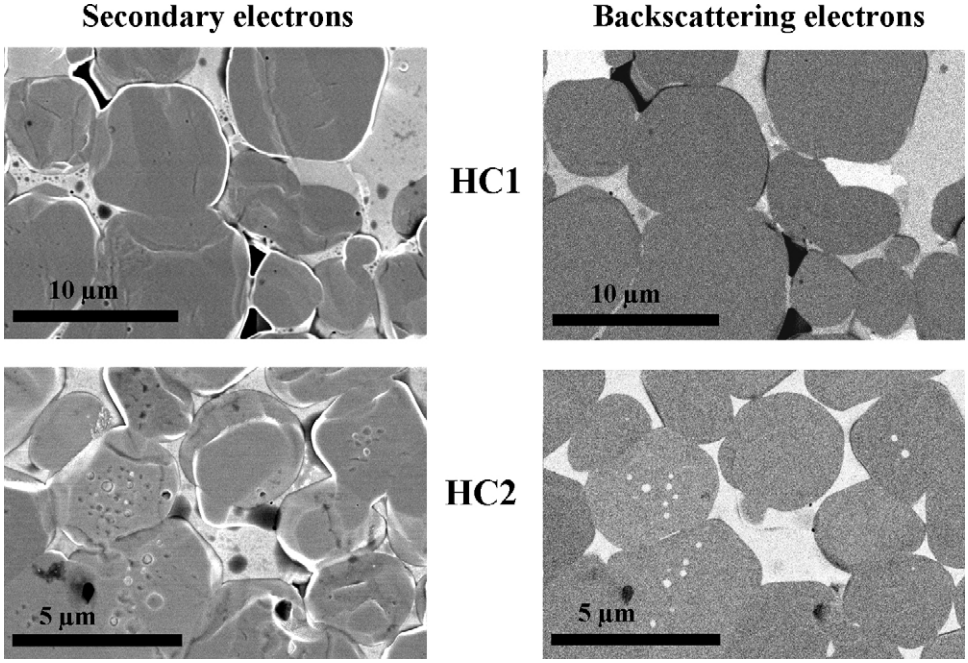

Fig. 10. HRSEM micrographs corresponding to cermets HC1 and HC2 taken with secondary and backscattering electrons. The lighter contrast corresponds to the binder phase.

round particles without a binder phase inside were observed that put forward a growth characterized by a solution–reprecipitation process but not by coalescence. This fact is clearly seen when HRSEM images of cermets HC1 and HC2 are compared (Fig. 10). The binder phase forming small particles inside the ceramics (white contrast) was only observed in cermet HC2 (using backscattering electrons). Previous work has shown that increasing the nitrogen ratio in titanium carbonitride reduces titanium solubility and then grain growth of hard particles.[1] However, the abnormal growth observed in cermet HC1 (the particle ratio size is nearly 2:1 comparing with cermet HC2, see Fig. 10) was inconsistent with a lower solubility of the hard ceramic and with the high amount of titanium present in the binder, as both circumstances should have inhibited grain growth.

However, it has been shown in WC–Co hard metals obtained from fine powders that before the liquid state was generated, a considerable hard particle growth was produced.[41] Recently, Kang et al.[42] have observed in ultrafine powdered Ti(C, N)-Ni cermets an extensive solid-state growth and coalescence of hard particles in the temperature range of 800–900 °C prior to liquid formation. This process occurred in a short period of time and particles with spherical microstructure were obtained. It would be then possible that the microstructure observed in cermet HC1 was the result of an extensive growth in the solid-state regime. This solid-state growth could be favoured by the nanometric character of ceramic powder obtained by MSR, while a decreasing wettability of ceramic particles when TiC_xN_{1-x} is richer in nitrogen and titanium is present in the binder. Some particle contiguity and shape of coarsened particles noted in the SEM micrograph of cermet HC1 (Fig. 7) could also be an indication of a coalescence behaviour in the solid-state. This solid-state coalescence must be followed by shape rounding to obtain the final observed microstructure.

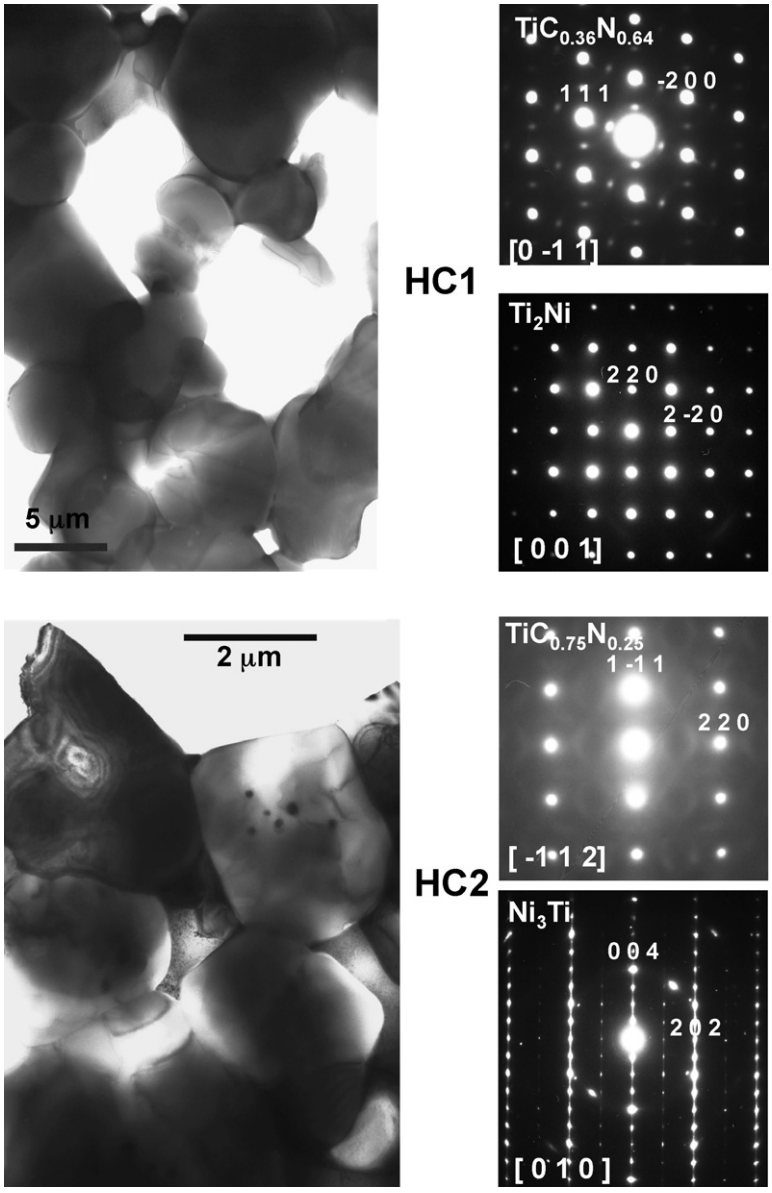

Fig. 11. TEM micrographs and ED patterns of the ceramic and different binder phases corresponding to cermets HC1 and HC2.

The microstructure of cermets HC1 and HC2 has also been compared using TEM and ED experiments, which are presented in Fig. 11. TEM micrographs show the size difference for both samples. The ED study of the ceramic particles in cermet HC1 has shown two different features as can be seen along the [0 −1 1] zone axis, an additional periodic diffuse intensity distribution and some diffraction spots not belonging to the standard ED for TiC_xN_{1-x} (cubic system *Fm*-3*m* space). Both of these features are known to be caused by ordering of vacancies in the C/N cubic sublattice,[43] where {1 1 1}-type planes in the large range order state are alternately fully occupied and empty. They have alternatively high and low occupancy. This ED also exhibit curves of diffuse intensity passing through the carbonitride diffraction spots. This is a characteristic feature of the transition while passing from the short range to the large range order state. On the other hand, $NiTi_2$ (cubic *Fd*3*m*; JCPDS 18-0898) was identified as binder by ED analysis and the zone axes along [0 0 1] is presented. This result agrees with the X-ray diffraction data. ED patterns of sample HC2 have also shown diffuse scattering as can be seen in the [−1 1 2] zone axis, which is related with the short range order produced by the C/N vacancies as in the HC1 sample. Ni_3Ti (hexagonal *P*63/*mmc*; JCPDS 75-0878) was found as binder and the [0 1 0] zone axis is presented.

4. Conclusions

MSR can be a powerful technique in obtaining powdered cermets based on titanium carbonitride. Synthesis can be performed in one step from the mixtures of elemental powders. For some starting mixtures, intermetallic phases constituted the cermet binder. A titanium carbonitride phase richer in carbon than the starting composition of raw powders was always obtained. MSR allows that metallic binder was homogeneously dispersed over ceramic particles. Both ceramic and binder phases present homogenous chemical composition and nanometric character after MSR synthesis.

After sintering by a pressureless method, the chemical composition characterization of cermets has consistently shown a titanium carbonitride phase richer in carbon than expected from stoichiometry of raw powders and a binder constituted by intermetallic phases. If metallic binder (Ni or Co) was added to the powder mixture prior to the MSR process, an even carbon-richer composition was obtained, which is consistent with the presence of a higher amount of Ti in the binder. There is a relationship between the stoichiometry of TiC_xN_{1-x} and the final titanium content in the binder phase after sintering. It must be noted that the incorporation of titanium to the binder in HC cermets occurred principally during the powder synthesis by MSR and not during sintering, as in the case of HCB cermets.

Microstructural characterization showed a bimodal size distribution for hard particles. Small spherical particles and larger faceted particles grown by a coalescence process were generally observed. Coalescence process (liquid-like coalescence of islands) generated the presence of binder phase inside hard particles. Particular microstructure found in cermets with a poorer carbon hard phase can be a consequence of a great extent of the grain growth in the solid-state regime. For the same gross composition, similar chemical composition for the hard and binder phases was found independently if the binder was submitted to a MSR process or blended with TiC_xN_{1-x} after MSR was performed. However, finer hard particles were obtained in the former case due to the inhibition of hard particle growth as a consequence of the presence of high amounts of titanium in the binder that reduced TiC_xN_{1-x} solubility. These preliminary results suggest that this new synthesis methodology coupled with the employ of more adapted sintering process would allow the fabrication of cermets with designed chemistry, microstructure and properties.

References

1. Ettmayer, P., Kolaska, H., Lengauer, W. and Dreyer, K., Ti(C, N) cermets—metallurgy and properties. *Int. J. Refract. Met. Hard Mater.*, 2000, **13**, 343–351.
2. Fukuara, M. and Mitami, H., Mechanism of grain growth in Ti(C, N)–Ni sintered alloys. *Powder Metall.*, 1982, **25**, 2.
3. Qi, F. and Kang, S., A study on microstructural changes in Ti(C, N)–NbC–Ni cermets. *Mater. Sci. Eng. A*, 1998, **251**, 276–285.
4. Zhang, S., Material development of titanium carbonitrides based cermets for machining application. *Key Eng. Mater.*, 1998, **521**, 138–140.
5. Pastor, H., Titanium-carbonitride-based alloy for cutting tools. *Mater. Sci. Eng. A*, 1988, **105–106**, 401–409.
6. Zhang, S., Titanium carbonitride-based cermets: processes and properties. *Mater. Sci. Eng. A*, 1993, **163**, 141–148.
7. Ritcher, V. and Ruthendorf, M., Composition, microstructure, properties and cutting performance of cermets. In *Proceedings of Euro PM '99, Advances in Hard Materials Production*, 1999, pp. 226–229.
8. Kieffer, R., Ettmayer, P. and Freudhofmeier, M., *Modern Development in Powder Metallurgy*, *vol. 5*, ed. H. H. Hausner. Plenum Press, New York, 1971.
9. Chen, L., Lengauer, W. and Dreyer, K., Advances in modern nitrogen-containing hardmetals and cermets. *Int. J. Refract. Met. Hard Mater.*, 2000, **18**, 153–161.
10. Vicenzi, B., Risso, L. and Calzavarini, R., High performance milling and gear hobbing by means of cermet tools with a tough (Ti, W, Ta)(C, N)–Co, Ni, W composition. *Int. J. Refract. Met. Hard Mater.*, 2001, **19**, 11–13.
11. Jeon, E. T., Joardar, J. and Kang, S., Microstructure and tribo-mechanical properties of ultrafine Ti(CN) cermets. *Int. J. Refract. Met. Hard Mater.*, 2002, **20**, 207–211.
12. Suryanarayana, C., Mechanical alloying and milling. *Prog. Mater. Sci.*, 2001, **46**, 1–184.
13. Ye, G. T. and Troczynski, T., Mechanochemical activation-assisted low-temperature synthesis of $CaZrO_3$. *J. Am. Ceram. Soc.*, 2007, **90**, 287–290.
14. Cordoba, J. M., Murillo, R., Alcala, M. D., Sayagues, M. J. and Gotor, F. J., Synthesis of TiN/Si_3N_4 composite powders by mechanically activated annealing. *J. Mater. Res.*, 2005, **20**, 864–873.
15. Ren, R. M., Yang, Z. G. and Shaw, L. L., Synthesis of nanostructured TiC via carbothermic reduction enhanced by mechanical activation. *Scr. Mater.*, 1998, **38**, 735–741.
16. Bernard, F., Souha, H. and Gaffet, E., Enhancement of self-sustaining reaction Cu_3Si phase formation starting from mechanically activated powders. *Mater. Sci. Eng. A*, 2000, **284**, 301–306.
17. Riley, D. P., Kisi, E. H. and Phelan, D., SHS of Ti_3SiC_2: ignition temperature depression by mechanical activation. *J. Eur. Ceram. Soc.*, 2006, **26**, 1051–1058.
18. Tsuchida, T. and Yamamoto, S., Mechanical activation assisted self-propagating high-temperature synthesis of ZrC and ZrB_2 in air from Zr/B/C powder mixtures. *J. Eur. Ceram. Soc.*, 2004, **24**, 45–51.
19. Takacs, L., Self-sustaining reactions induced by ball milling. *Prog. Mater. Sci*, 2002, **47**, 355–414.

20. Yen, B. K., Aizawa, T. and Kihara, J., Synthesis and formation mechanisms of molybdenum silicides by mechanical alloying. *Mater. Sci. Eng. A*, 1996, **220**, 8–14.
21. Córdoba, J. M., Sayagués, M. J., Alcalá, M. D. and Gotor, F. J., Synthesis of titanium carbonitride phases by reactive milling of the elemental mixed powders. *J. Am. Ceram. Soc.*, 2005, **88**(7), 1760–1764.
22. Córdoba, J. M., Sayagués, M. J., Alcalá, M. D. and Gotor, F. J., Monophasic nanostructured powders of Nb, Ta and Hf carbonitride phases synthesized by mechanically induced self-propagating reaction. *J. Am. Ceram. Soc.*, 2007, **90**(2), 381–387.
23. Córdoba, J. M., Sayagués, M. J., Alcalá, M. D. and Gotor, F. J., Monophasic $Ti_yNb_{1-y}C_xN_{1-x}$ nanopowders obtained at room temperature by MSR. *J. Mater. Chem.*, 2007, **17**(7), 650–653.
24. Rodriguez-Carvajal, J., FULLPROF, February 2006 version, ILL.
25. Kim, G. H., Kim, H. S. and Kum, D. W., Determination of titanium solubility in alpha-aluminum during high energy milling. *Scr. Mater.*, 1996, **34**, 421–428.
26. Lavergne, O., Robaut, F., Hodaj, F. and Allibert, C. H., Mechanism of solid-state dissolution of WC in Co-based solutions. *Acta Mater.*, 2002, **50**, 1683–1692.
27. Huang, J. Y., Ye, L. L., Wu, Y. K. and Ye, H. Q., Microstructure investigation on explosive Ti(or Ni)/TiC-composite formation reaction during mechanical alloying. *Acta Mater.*, 1996, **44**, 1781–1792.
28. Wong, J., Larson, E. M., Holt, J. B., Waide, P. A., Rupp, B. and Frahm, R., Time resolved X-ray diffraction study of solid combustion reactions. *Science*, 1990, **249**, 1406–1409.
29. Han, J. C., Zhang, X.-H. and Wood, J. V., In-situ combustion synthesis and densification of TiC–*x*Ni cermets. *Mater. Sci. Eng. A*, 2000, **280**, 328–333.
30. Burkes, D. E., Gottoli, G., Moore, J. J. and Yi, H. C., Production of Ni_3Ti–TiC_x intermetallic-ceramic composites employing combustion synthesis reactions. *Metall. Mater. Trans. A*, 2006, **37**, 1045–1053.
31. Burkes, D. E., Gottoli, G., Yi, H. C. and Moore, J. J., Combustion synthesis and mechanical properties of dense NiTi–TiC intermetallic-ceramic composites. *Metall. Mater. Trans. A*, 2006, **37**, 235–242.
32. Zhou, L. Z., Guo, J. T. and Fan, G. J., Synthesis of NiAl–TiC nanocomposite by mechanical alloying elemental powders. *Mater. Sci. Eng. A*, 1998, **249**, 103–108.
33. Fan, G. J., Quan, M. X., Hu, Z. Q., Eckert, J. and Schultz, L., In-situ explosive formation of $NbSi_2$-based nanocomposites by mechanical alloying. *Scr. Mater.*, 1999, **41**, 1147–1151.
34. Alvarez, M. and Sanchez, J. M., Spark plasma sintering of Ti(C, N) cermets with intermetallic binder phases. *Int. J. Refract. Met. Hard Mater.*, 2007, **25**, 107–111.
35. Tiegs, T. N., Schroeder, J. L., Montgomery, F. C. and Baker, D. L., Sintering and evolution of microstructure in TiC–Ni_3Al cermets. *Int. J. Powder Met.*, 2000, **36**, 46.
36. Tiegs, T. N., Alexander, K. B., Plucknett, K. P., Menchhofer, P. A., Becher, P. F. and Waters, S. B., Ceramic composites with a ductile Ni_3Al binder phase. *Mater. Sci. Eng. A*, 1996, **209**, 247.
37. Kang, S., Stability of N in Ti(C, N) solid solutions for cermets applications. *Powder Metall.*, 1997, **40**, 13.
38. Jung, I. J., Kang, S., Jhi, S. H. and Ihm, J., A study of the formation of Ti(C, N) solid solutions. *Acta Mater.*, 1999, **47**, 3241.
39. Suryanarayanan Iyer, R. and Sastry, S. M. L., Consolidation of nanoparticles-development of a micromechanistic model. *Acta Mater.*, 1999, **47**, 3079.
40. Mari, D., Bolognini, S., Feusier, G., Cutard, T., Verdon, C., Viatte, T. and Benoit, W., TiMoCN based cermets. Part I: Morphology and phase composition. *Int. J. Refract. Hard Met.*, 2003, **21**, 37.
41. Allibert, C. H., Sintering features of cemented carbides WC–Co processed from fine powders. *Int. J. Refract. Met. Hard. Mater.*, 2001, **19**, 53.
42. Kang, Y., Lee, G. H. and Kang, S., Growth of ultrafine Ti(CN) particles in Ti(CN)–Ni cermets. *Scr. Mater.*, 2007, **56**, 133.
43. Bursik, J. and Weatherly, G. C., Ordering of substoichiometric d-TiC_x phase. *Phys. Status Solidi (a).*, 1999, **174**, 327.